Some Investigations of $S_5N_5^+$ Compounds; *X*-Ray Crystal Structure of $[S_5N_5]Cl$†

Arthur J. Banister,* Zdenek V. Hauptman, and Aidan G. Kendrick
Department of Chemistry, University of Durham, Science Laboratories, South Road, Durham DH1 3LE
Ronald W. H. Small
Department of Chemistry, University of Lancaster, Bailrigg, Lancaster LA1 4YA

Aluminium chloride is removed from cyclopenta(azathienium) tetrachloroaluminate by tetrahydrofuran to give pure $[S_5N_5]Cl$ and this reacts with aqueous tetrafluoroboric acid to give $[S_5N_5][BF_4]$. Cyclic voltammograms of $[S_5N_5]Cl$ in liquid SO_2 show reduction of $S_5N_5^+$ at $E_{p/2}^{red}$ = 0.34 V *vs.* a saturated calomel electrode; the process is reversible. Cyclic voltammograms of $[S_5N_5][BF_4]$ in MeCN were more complex and a mechanism for this electroreduction is proposed. Electrodeposition of $(SN)_x$ on platinum-foil and on $(SN)_x$-film cathodes was achieved by potentiostatic electrolysis. $[S_5N_5]Cl$ crystallizes in the monoclinic space group $C2/c$, with a = 7.98(1), b = 14.37(1), c = 7.30(1) Å, β = 97.15(5)°, and Z = 4. 1 366 Observed reflections were refined to R = 0.054. The mean bond angles are NSN 111.3 and SNS 140.2°. Three of the five unique S–N distances are 158.2 pm but two [S(2)–N(2) 156.5, S(3)–N(3) 159.8 pm] are affected by short S · · · Cl contacts [3.277(1) and 3.148(1) Å at S(2) and 3.243(1) and 3.279(1) Å at S(3)]. Strain in the azulene-shaped cation arising from cation–anion interactions can be detected by comparing bond distances and angles with the strain-free values deduced from either bond distance–bond angle correlation functions or MNDO calculations.

The monocyclic cation $S_5N_5^+$ is the 14-π member of the Hückel set of cyclothiazenes. Most reported salts contain large counter ions [*e.g.* $S_3N_3O_4^-$,[1] $SnCl_5(OPCl_3)^-$,[2] $AlCl_4^-$,[3] $GaCl_4^-$,[4] $Ga_2Cl_7^-$ [4]] and, with colourless anions, the salts are yellow. The chloride, however, is red indicating either significant cation–anion interaction and/or a different cation conformation. Two isomers of $S_5N_5^+$ have been reported from *X*-ray structure determinations (with an azulene[1,2,4] or 'heart' shape[3,4]). The apparent heart shape may well arise from cation size disorder,[5] but since MNDO calculations[6] show that the two shapes probably have similar energy, genuine isomerism is still possible. We have therefore determined the structure of $S_5N_5^+Cl^-$ and find significant cation–anion interaction associated with the re-entrant portion of an azulene-type $S_5N_5^+$ ring. We also report a new preparation of $[S_5N_5]Cl$ from $[S_5N_5][AlCl_4]$ and tetrahydrofuran (thf) and describe a solvate, $[S_5N_5]Cl{\cdot}SO_2$.

We have investigated further the electrochemical reduction of $S_5N_5^+$ ($S_5N_5^+Cl^-$–SO_2, $S_5N_5^+BF_4^-$–$LiClO_4$–MeCN) to the conducting polymer $(SN)_x$[7] on both a macro- and micro-electrode scale. In a broader context, the purpose of this investigation was (*i*) to elucidate the reaction mechanism at the electrode surfaces under various conditions, (*ii*) to work out a preparation method for pure polycrystalline $(SN)_x$ (in quantities of tenths of a gram per batch) suitable as a source for vacuum deposition of electrically conductive films, and (*iii*) to explore the possibility of a direct electrochemical coating with compact layers of $(SN)_x$ (10^2—10^4 Å thick) on conducting or semi-conducting substrates.

† Cyclopenta(azathienium) chloride.

Supplementary data available (No. SUP 56661, 4 pp.): thermal analyses, i.r. spectra. See Instructions for Authors, *J. Chem. Soc., Dalton Trans.*, 1987, Issue 1, pp. xvii—xx.

Non-S.I. units employed: cal = 4.184 J, eV = 1.60 × 10^{-19} J, atm = 101 325 Pa, mmHg = 133 Pa, in = 2.54 × 10^{-2} m.

Results and Discussion

Cyclopenta(azathienium) chloride, $[S_5N_5]Cl$, originally obtained by melting S_4N_4 and $(NSCl)_3$ at 65 °C,[8] was first prepared in a pure, more stable state by reacting $[S_5N_5][FeCl_4]$ and CsF followed by extraction with MeCN.[7] These two methods have been examined further and compared with a third and new route in which thf abstracts $AlCl_3$ from $[S_5N_5][AlCl_4]$.

The S_4N_4–$(NSCl)_3$ route, although starting from easily preparable materials, requires the hazardous[9] operation of grinding together S_4N_4 and $(NSCl)_3$ in a dry-box. We found that the ease of melting of the intimate mixture of S_4N_4 and $(NSCl)_3$ (and hence the yield of $[S_5N_5]Cl$) depended strongly on the degree of grinding and the purity of the starting materials; pure S_4N_4–$(NSCl)_3$ mixtures required higher temperatures and did not achieve homogeneous melting. The reaction of $[S_5N_5][FeCl_4]$ with CsF [equation (1)] at room temperature (15 °C) gave good quality $[S_5N_5]Cl$ after purification by exhaustive extraction with acetonitrile; the yield was 69%. The new preparation from $[S_5N_5][AlCl_4]$ and thf [equation (2)] produces good quality $[S_5N_5]Cl$ at the same temperature in a shorter time with less effort and in higher yield (> 80%).

$$[S_5N_5][FeCl_4] + 3CsF \xrightarrow{SO_2} [S_5N_5]Cl + 3CsCl + FeF_3\downarrow \quad (1)$$

$$[S_5N_5][AlCl_4] + thf \longrightarrow [S_5N_5]Cl\downarrow + AlCl_3{\cdot}thf \quad (2)$$

We found a marked difference in stability of the $[S_5N_5]Cl$ obtained from these three routes; that obtained from the melt decomposes after a few days at room temperature whereas that obtained by either of the routes from $[S_5N_5][MCl_4]$ is, after purification, stable for months at room temperature.

Pure $[S_5N_5]Cl$ is a scarlet-red microcrystalline solid, soluble in SO_2, HCOOH, and Me_2SO, very sparingly soluble in acetonitrile and readily converted to $[S_5N_5][BF_4]$ by aqueous HBF_4. The crystals formed, on concentrating the solution of $[S_5N_5]Cl$ in SO_2, were pale yellow in the presence of the mother-

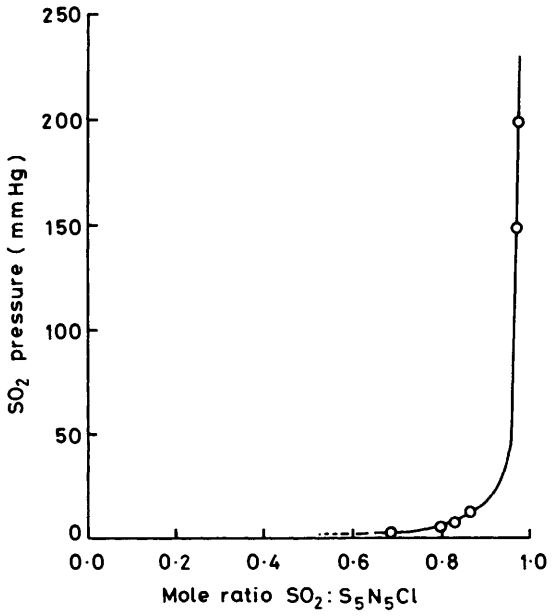

Figure 1. Quasi-equilibrium partial pressure of SO_2 at 2 °C in the system $SO_2(g)$–$[S_5N_5]Cl(s)$ as a function of the mole ratio

liquor, but they turned red on prolonged pumping. Vapour pressure data indicate that this yellow crystalline solid is a metastable solvate, $[S_5N_5]Cl{\cdot}SO_2$.*

Tensimetric titration of pure solid $[S_5N_5]Cl$ with SO_2 at 2 °C (Figure 1) showed that, although the system (3) did not attain

$$[S_5N_5]Cl(s) + nSO_2(g) \rightleftharpoons [S_5N_5]Cl{\cdot}nSO_2(s) \quad (3)$$

complete equilibrium on a convenient time-scale, the solvate formed had a 1:1 stoicheiometry. Because of the slow equilibration the value of ΔH(solvation) (as a function of $p_{SO_2}^{eq}$ and absolute temperature) was unobtainable. The chloride ion is probably converted to the known[10] chlorosulphinate ion, SO_2Cl^-.

The $S_5N_5^+$ cation has the S:N ratio which is appropriate for reduction to the superconducting polymer $(SN)_x$; the use of a chloride or fluoroborate salt avoids the possibility of contamination by metallic species.

Cyclic Voltammetric Studies of the $S_5N_5^+$ *Ion.*—Further to our report of the electrochemical reduction of $[S_5N_5]Cl$ to $(SN)_x$ in liquid SO_2,[7] we investigated the mechanism of reaction using cyclic voltammetry. The results indicated that direct electrocrystallization might be achieved by electroreduction of $[S_5N_5][BF_4]$ in acetonitrile using a platinum or $(SN)_x$-coated cathode; the mechanism of this reaction was also studied using cyclic voltammetry. The results are discussed below.

(*a*) *In liquid* SO_2. Although several earlier attempts were made to apply cyclic voltammetry to SO_2 solutions,[11] it was not until 1979 that Tinker and Bard[12] developed successful procedures for obtaining cyclic voltammograms in this solvent. They used tertiary butyl ammonium salts as background

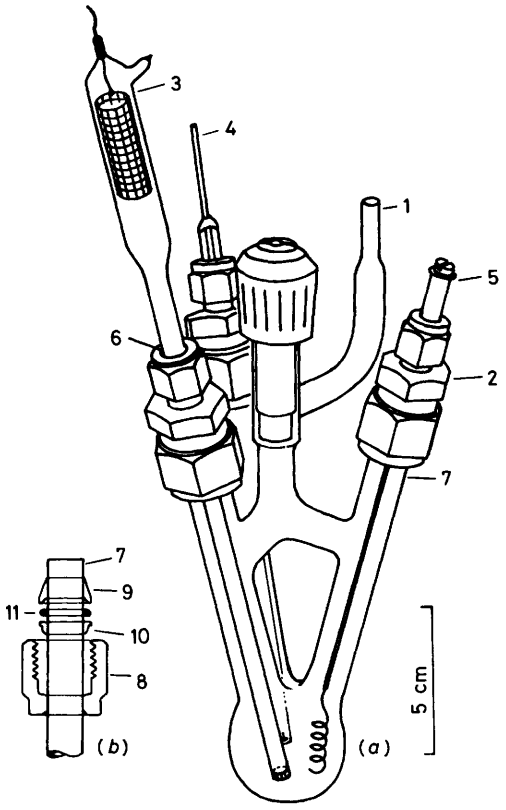

Figure 2. (*a*) Three-electrode cell designed for c.v. in liquid SO_2 and non-aqueous solvents: (1) attachment to vacuum and nitrogen lines; (2) 'Swagelok' $\frac{1}{2}$- to $\frac{1}{4}$-in reducers to provide an airtight union with (3) the reference electrode, (4) the working electrode, (5) the auxiliary electrode, and (6) $\frac{1}{4}$-in insertion port for the r.e. (3); (*b*) 'Swagelok' union to (7) the $\frac{1}{2}$-in precision Pyrex tubing, modified to improve the vacuum and pressure seal; (8) compression nut, (9) poly(tetrafluoroethylene) (ptfe) front ferrule, (10) ptfe back ferrule (reversed), and (11) added Viton O-ring (internal diameter $\frac{1}{16} \times \frac{3}{8}$ in)

electrolytes, and a quasi-reference electrode, Ag/Ag^+, which was refilled each time the cell was filled; the difficulty in reproducing the exact volume of solution in the cell resulted in a reproducibility of only ±50 mV in the potential of the reference electrode. An additional inconvenience was that the electrochemical cell was constructed with cone and socket joints which necessitated a low (−40 °C) experimental temperature in order to reduce the vapour pressure of SO_2.

The experiments described here have overcome some of the difficulties experienced by other workers. The cell (Figure 2), constructed with Swagelok fittings, withstood pressures of up to 3 atm and so it could be used at ambient temperatures. The reference electrode was completely filled with acetonitrile solution and hence (because of the incompressibility of liquids) it could also be used in pressurized solutions; a dense sintered Pyrex diaphragm limited inter-diffusion of the different solvents. Since the electrode was not refilled between each experiment, its potential remained remarkably stable (±5 mV). Although some potential drift was observed (from frequent checks against a saturated calomel electrode, s.c.e.) over periods of several months, measured values could still be compared by conversion to the s.c.e. scale.

In Figures 3 and 4 and in all subsequent discussion, the potential scale, although measured against the Ag/Ag^+ electrode, has been converted to the s.c.e. scale. The major reduction peak at $E_{p/2}^{red} = 0.34$ V can be assigned to the reduction of the $S_5N_5^+$ ion (*cf.* $E_{p/2}^{red} = +0.46$ V for

* When $[S_5N_5]Cl$ was left in contact with liquid SO_2 for several weeks a complex reaction took place: $S_4N_4O_2$ and $[S_4N_3][SO_3Cl]$ were isolated from the saturated solution of $[S_5N_5]Cl$ in SO_2 whereas $[S_4N_5][SO_3Cl]$ (red crystals), $[S_4N_3][SO_2Cl]$ (yellow crystals), $[S_6N_4]Cl_2$, and $SOCl_2$ were identified as products from a sealed ampoule containing *ca.* 1 g $[S_5N_5]Cl$ and 1 g SO_2. The products were identified by i.r. spectroscopy.

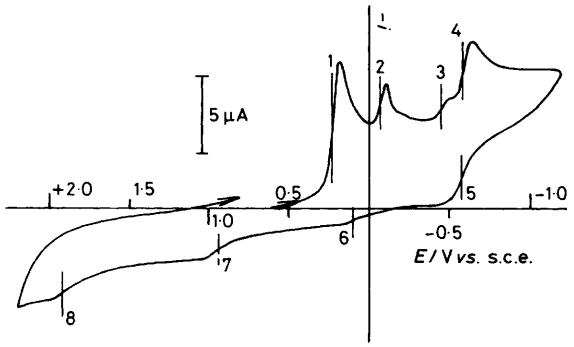

Figure 3. A typical cyclic voltammogram for $[S_5N_5][BF_4]$ (10^{-3} mol dm^{-3}) in $[NBu_4][BF_4]$ (0.2 mol dm^{-3})–MeCN; temperature 0 °C, potential sweep rate 100 mV s^{-1}. The figures, which denote half-wave potentials, relate to Table 1 and Figure 4 (*a*)—(*d*)

$[S_5N_5][FeCl_4]$ in methylene chloride).[13] Unlike the earlier study by Fritz and Bruchhaus[13] of $[S_5N_5][FeCl_4]$ in methylene chloride, the reduction of $[S_5N_5]Cl$ in SO_2 was found to be a reversible process with $E^{ox}_{p/2} = +0.30$ V, a half-peak potential difference of 40 mV, compared to the 56 mV allowed for a reversible process.[14] The further large oxidation peak at $E^{ox}_{p/2} = +1.32$ V was assigned to oxidation of Cl^- (*cf.* +1.3 V *vs.* Ag/AgCl).[15] The very small oxidation peak at $E^{ox}_{p/2} = +1.08$ V cannot be assigned unambiguously but may arise from anodic breakdown of a microlayer of $(SN)_x$ formed in the initial reduction process since the anodic breakdown potential of $(SN)_x$ electrodes has been reported as +1 V.[16]

Anodic breakdown on the cyclic voltammogram occurred at *ca.* +2.5 V and is assigned to the oxidation of the BF_4^- ion, presumably with formation of BF_3 and SO_2F_2 (by reaction with solvent). The anodic breakdown observed in this system is at less positive potentials than have been reported for BF_4^--containing electrolytes in liquid SO_2;[12] it is not clear why this should be the case. The cathodic breakdown occurs at *ca.* −0.16 V and can be assigned to the reduction of SO_2 to $SO_2^{\bullet -}$.[15,17] The proximity of the $S_5N_5^+$ reduction to the SO_2 reduction implies that, using a non-potentiostatic current source, the bulk electroreduction of $S_5N_5^+$ is probably mediated by $SO_2^{\bullet -}$ or $S_2O_4^{\bullet -}$. In addition to accounting for the powdery nature of the cathodic deposit and turbidity of the electrolyte solution, this mechanism would also account for the observed constancy of current and potential, even when a non-galvanostatic current source was used. Since a major research aim was to achieve electrocrystallization of $(SN)_x$, it was decided to investigate the $S_5N_5^+$ electroreduction in an 'electro-inert' solvent (such as acetonitrile). This was to ensure that discharge of the cation occurred at the cathode surface, enabling more precise control of conditions.

(*b*) *In acetonitrile.* In order to examine the electroreduction of $S_5N_5^+$ to $(SN)_x$ in an electrochemically inert solvent and more especially to investigate the possibility of electrocrystallization and deposition of compact layers, a cyclic voltammetric study of $[S_5N_5][BF_4]$ in acetonitrile was undertaken as a preliminary to bulk electrolysis. Both acetonitrile and the BF_4^- ion are recognised to be particularly electro-inert.[14] A typical cyclic voltammogram is illustrated in Figure 3 and voltammograms recorded at different temperatures are illustrated in Figure 4. A mechanism for the electroreduction of $S_5N_5^+$ in acetonitrile is proposed on the basis of the voltammograms obtained and published data; peak numbers referred to in the text correspond to those in Figure 3 and the half-peak reduction potentials are summarised in Table 1.

The first peak (1, $E^{red}_{p/2} = +0.23$ V) is assigned to the reduction of the $S_5N_5^+$ ion (*cf.* $E^{red}_{p/2} = +0.46$ V for

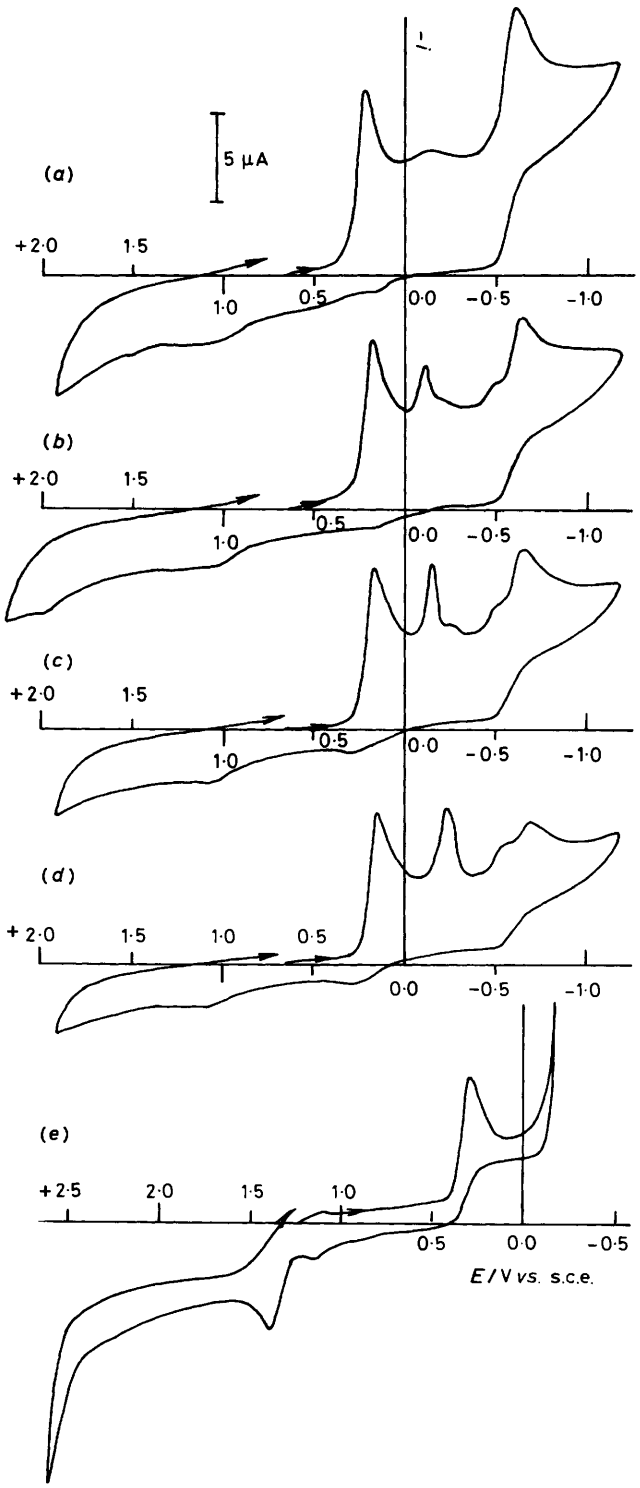

Figure 4. Cyclic voltammograms for $[S_5N_5][BF_4]$ (10^{-3} mol dm^{-3}) in $[NBu_4][BF_4]$ (0.2 mol dm^{-3})–MeCN (*a*)—(*d*) and $[S_5N_5]Cl$ (10^{-3} mol dm^{-3}) in $[NBu_4][BF_4]$ (0.2 mol dm^{-3})–liquid SO_2 (*e*) at a platinum electrode: (*a*) 15.5, (*b*) 0, (*c*) −6, (*d*) −18.5, (*e*) 0 °C. Potential sweep rate 100 mV s^{-1}

$[S_5N_5][FeCl_4]$ in methylene chloride[13]) although in this system no corresponding oxidation peak is observed and hence the process is irreversible [unlike (*a*) above].

The height of the second peak (2, $E^{red}_{p/2} = -0.08$ V) depends

Table 1. Cyclic voltammetric data ($E_{p/2}$/V)* for $[S_5N_5][BF_4]$ in $[NBu_4][BF_4]$ (0.2 mol dm^{-3})–MeCN

	Peak							
Temp. (°C)	1	2	3	4	5	6	7	8
15.5	+0.28	−0.06		−0.54	−0.55	+0.10	+0.94	
0.0	+0.23	−0.08	−0.47	−0.59	−0.59	+0.13	+0.94	+1.90
−6.0	+0.21	−0.12	−0.46	−0.58	−0.58	+0.18	+0.96	
−18.5	+0.19	−0.19	−0.51	−0.59	−0.61	+0.19	+0.98	

* All data recorded at scan rate of 100 mV s^{-1}, sensitivity 20 μA V^{-1}.

strongly on temperature; at room temperature, it is present only as a weak, broad feature but at lower temperatures the peak became progressively sharper and more intense, until at −18.5 °C it was the same height as peak 1. A small shoulder appeared on the cathodic side of the peak at 0 and −6 °C but was not present at 15.5 and −18.5 °C. These observations may be rationalized by assigning peak 2 to the reduction of a short-lived neutral species produced by fragmentation of the $S_5N_5^{\bullet}$ radical (see below). The cathodic shoulder is probably closely related, but since it shows a non-linear dependence on temperature, it is difficult to speculate further on its origin.

The reduction peaks 3 and 4 ($E_{p/2}^{red} = -0.47$ and −0.59 V respectively) and the oxidation peak 5 ($E_{p/2}^{ox} = -0.59$ V) may all be assigned to the reversible reduction of S_4N_4. Peak 3 corresponds to the prewave observed by Chivers and Hojo[18] in their polarographic study of S_4N_4. They found that the height of the prewave increased at low temperature and depended on the supporting electrolyte, but not on the concentration of S_4N_4 and so concluded that the prewave arose from adsorption phenomena. Peaks 4 and 5 correspond to the reduction of S_4N_4 to $S_4N_4^-$ and its reoxidation respectively.[18] Addition of a small quantity of S_4N_4 to the system resulted in a marked increase in the heights of peaks 4 and 5. The very small oxidation peaks (6—8) presumably correspond to oxidation of species formed in the reduction processes. As before, peak 7 ($E_{p/2}^{ox} = +0.94$ V) may correspond to the anodic breakdown of an $(SN)_x$ microlayer,[16] but more specific assignments are not possible.

These data usefully complement those reported by Fritz and Bruchhaus[13] for the electroreduction of $[S_5N_5][FeCl_4]$, who found reduction peaks at $E_{p/2}^{red} = +0.46$ and −0.5 V *vs.* s.c.e. (corresponding to peaks 1 and 4 in the present work). The first, irreversible peak was assigned to the reduction of $S_5N_5^+$ and the second, reversible peak was assigned to the reduction of other, unspecified sulphur–nitrogen species. Intermediate peaks in that system were masked by the reversible reduction of $FeCl_4^-$.

The overall reaction mechanism inferred from our cyclic voltammetric data and subsequent bulk electrolyses can be summarized in the Scheme. The $S_5N_5^+$ ion is discharged to form the transient $S_5N_5^{\bullet}$ radical. This may either (*i*) ring-open to form $(SN)_x$, or (*ii*) cleave to form two neutral species (denoted S_nN_n and S_mN_m); these could be SN* and S_4N_4 (linear) or S_2N_2 (linear or cyclic) and $S_3N_3^{\bullet}$ (linear or cyclic). One of these species is stabilized at low temperatures and is subsequently reduced to an anion (peak 2); the other may rearrange to form either an $(SN)_x$ deposit or S_4N_4 (cyclic). At higher temperatures, no stabilization occurs and both species rearrange without significant further reduction. Since the observed current yield of $(SN)_x$ in bulk electrolysis experiments in this system is in the region of 40—50% and since $S_3N_3^-$ is a stable species, the cleavage of the $S_5N_5^{\bullet}$ radical to linear S_2N_2 and cyclic $S_3N_3^{\bullet}$ seems to be the most likely path. Cyclic S_2N_2 does not appear to be an intermediate in the reduction process since no peak corresponding to its reduction {$E_{p/2}^{red} = -0.85$ V, $E_{p/2}^{ox} = 0.1$ V; S_2N_2 (*ca.* 10^{-3} mol dm^{-3}), $[NBu_4][BF_4]$ (0.1 mol dm^{-3}) in MeCN at 16.5 °C}[19] is present in the voltammograms. Finally,

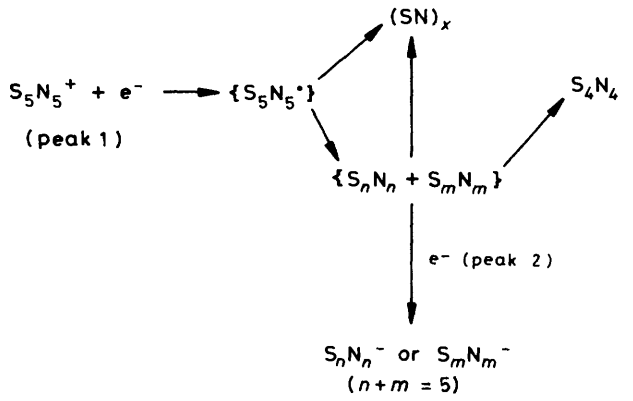

Scheme.

it is worth noting that processes (*i*) and (*ii*) may occur simultaneously, with temperature-determined rate constants. In principle it is possible to confirm the mechanism by *in situ* e.s.r. experiments but in practice these may be difficult to achieve, since no radical species were detected in the $[S_5N_5][FeCl_4]$–CH_2Cl_2 system[13] and no radicals were detectable in an *in situ* electrolysis of $[S_5N_5]Cl$ in liquid SO_2.*

With knowledge of the reduction potential of $S_5N_5^+$, it became possible to attempt potentiostatically controlled electrocrystallization of $(SN)_x$.

Potentiostatic Electrolysis of a Solution of $[S_5N_5][BF_4]$.—This was carried out in 0.1 mol dm^{-3} $LiClO_4$–MeCN using bright platinum electrodes at a potential of −0.26 V *vs.* a specially constructed Ag/Ag^+ reference electrode (3, Figure 2) which in turn had a potential of +0.26 V *vs.* s.c.e., yielded a bronze coloured compact deposit. Examination of this deposit under a scanning electron microscope (s.e.m.) revealed microcrystalline nodules [Figure 5(*a*)].

In another experiment with an electrolyte of the same composition we employed a vacuum-deposited layer of $(SN)_x$ on glass as a working electrode (w.e.). The layer (*ca.* 1.5 μm thick) had a bright gold metallic lustre and an examination with a polarising microscope (×400) showed randomly oriented crystallites with average dimensions *ca.* 5 μm. Reflection electron diffractography (r.e.d.) produced a distinct arc pattern with periodicities of 3.26 Å [distance between ($\bar{1}02$) planes] and hence confirmed that the crystallites had their ($\bar{1}02$) planes oriented parallel with the glass surface.[20,21] In this experiment we attempted an epitaxial electrocrystallization. With the potential at the w.e. set at 0 V *vs.* s.c.e. the current quickly steadied at 0.22 ± 0.02 mA. At first the optical appearance (high lustre) of the electrode remained unchanged indicating

* Experiment carried out by L. H. Sutcliffe and D. Bethell, University of Liverpool, School of Chemistry.

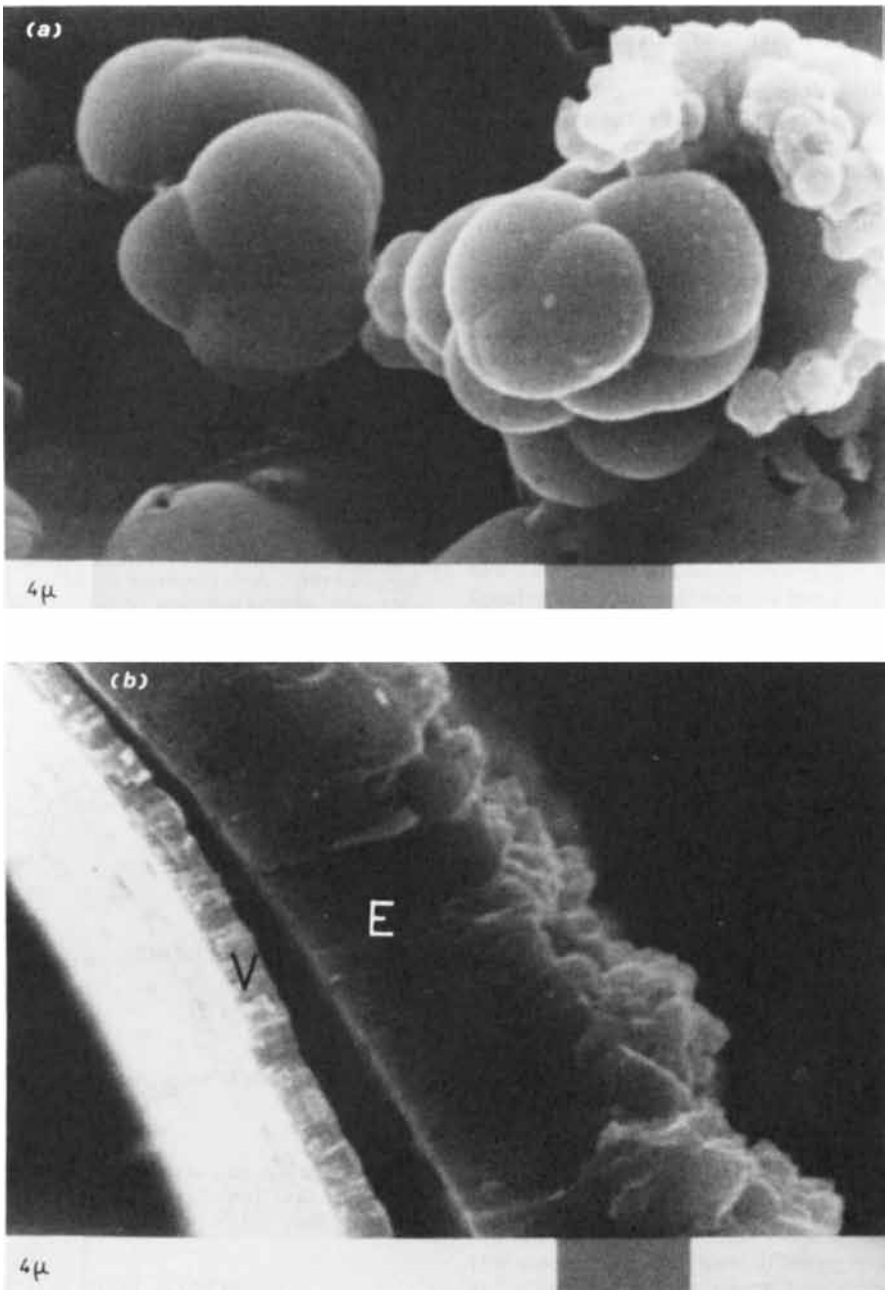

Figure 5. S.e.m. photographs of $(SN)_x$ obtained by electrochemical reduction (4 μm marker is shown bottom right). (*a*) Electrodeposited $(SN)_x$ on platinum cathode from $[S_5N_5][BF_4]$ in 0.1 mol dm^{-3} $LiClO_4$–MeCN solution at −0.26 V *vs.* s.c.e. (room temperature, r.t.). (*b*) Electrodeposited layer (E) of $(SN)_x$ (electrolyte as above, 0.0 V *vs.* s.c.e., r.t.) on a vacuum-deposited film of $(SN)_x$ (V). A fracture face across both separated layers is visible revealing a columnar texture of the E layer with grain boundaries approximately perpendicular to the substrate

that an epitaxial growth occurred. However, after 10 min the electrode surface roughened suddenly, presumably due to a secondary nucleation. The deposition continued, still at 0.22 mA, for a total of 4.5 h. The final deposit was washed with MeCN and dried *in vacuo*. Under an optical microscope (×40) it appeared microcrystalline with gold-bronzy sheen. Portions of the layer were lifted from the glass substrate (by gentle heating *in vacuo*). Once removed, the small fragments buckled while the larger ones (several mm) scrolled.

A scanning electron photograph [Figure 5(*b*)] shows a fracture face perpendicular across both layers. It is apparent that mechanical stress was responsible for the partial separation of the vacuum-deposited and the electrodeposited layers. We postulate that after the short initial epitaxial growth phase, new nuclei were formed; those with directions of the polymeric SN chains (and thus, the obvious direction of the fastest growth) oriented approximately perpendicular to the electrode surface, took over the control of further growth. [Note the direction of the grain boundaries in Figure 5(*b*).] As a consequence, a lattice mismatch generated mechanical stress. The average thickness of the electrodeposited layer, which was nearly uniform over the total conducting area (*ca.* 2 cm^2) of the $(SN)_x$ electrode, was 8 μm. A thickness of 16 μm would have corresponded to 100% current yield for a cathode reaction $S_5N_5^+ + e^- \longrightarrow \frac{5}{x}(SN)_x$. Thus, a current yield of *ca.* 50% was achieved.

The layer deposited on the $(SN)_x$-coated electrode had a higher degree of crystallinity than that deposited on bright platinum; as shown in Figure 5(*b*), the microcrystals on the coated electrode had dimensions *ca.* 8 × 4 μm compared with 5 × 5 μm on the bright platinum. The influence of electrode surface on the polymer crystallinity indicates that with an appropriate choice of electrode material it should be possible to grow electrolytically single crystals of $(SN)_x$.

A test was carried out to demonstrate whether the electrochemically prepared microcrystalline $(SN)_x$ can be used as a source material for fabrication of vacuum-deposited films of comparable quality to those prepared from $(SN)_x$ crystals (S_2N_2 route). A quantity (*ca.* 80 mg) of SO_2-washed microcrystals of $(SN)_x$ prepared by electrochemical reduction of $[S_5N_5]Cl$ in SO_2[7] was sublimed at 120—130 °C (in a sublimator described in ref. 22) on to glass slides. A uniform $(SN)_x$ coating *ca.* 1 μm thick with gold-bronzy metallic appearance was obtained in *ca.* 16 h. Optical reflectance and transmission spectra were measured (Figure 6) and were compared with literature data for the films from the classical (*i.e.*, from S_2N_2) poly(sulphur nitride).

For the transmission measurements one of the samples was heated to *ca.* 90 °C *in vacuo* and the film thickness was reduced to *ca.* 20%. The sample appeared uniformly blue. The reflectance spectrum was the same, within experimental error, as those reported in ref. 21. We also tested, using differential scanning calorimetry (d.s.c.), the thermal stability of $(SN)_x$ layers electrodeposited from $[S_5N_5][BF_4]$, and found that they were stable up to *ca.* 150 °C whereupon they decomposed non-explosively into elemental sulphur and nitrogen, *i.e.* only one exothermic peak (with maximum at 175 °C). The measured ΔH(decomp.) was -104 ± 5 kcal mol^{-1} of $(SN)_4$ (*cf.* ΔH_f for S_4N_4 is 128.0 ± 1.0 kcal mol^{-1}).[23] This thermal behaviour is in marked contrast with microcrystalline $(SN)_x$ obtained from the trimethylsilyl azide reduction of $(NSCl)_3$ in acetonitrile.[20] The d.s.c. record of the latter product showed that it was unstable with respect to S_4N_4 into which it exothermically converted at 110—130 °C with $\Delta H = -(4.8 \pm 0.2)$ kcal mol^{-1} for $(SN)_4$. This may be interpreted in terms of a higher degree of order and longer S–N chains in the electrochemical $(SN)_x$.

Structure of $[S_5N_5]Cl$.—Perhaps the most striking example of $S_5N_5^+$ disorder was described by Gillespie *et al.*[24] for $[S_5N_5][SbCl_6]$, in which the cation appears as a distorted azulene type ring. In $[S_5N_5]Cl$, however, there is no such disorder and in contrast to the approximate non-crystallographic *mm* symmetry of the $S_5N_5^+$ ion in previous structures,[24] a crystallographic C_2 axis passes through the apical atoms S(1) and N(3). Bond distances and angles within the cation are shown in Figure 7.The distances of the atoms from the mean plane are also indicated; the ten-membered azulene type ring is almost planar. Three of the five unique S–N distances [S(1)–N(1), S(2)–N(1), and S(3)–N(2)] have the same value within the limits of error whilst S(2)–N(2) and S(3)–N(3) are significantly below and above that value respectively.

The packing of the ions is shown in Figure 8(*a*) and (*b*); the cations are disposed in layers approximately parallel to (001), separated by $c/2$ with the chloride ions interleaved. There are four short S–Cl distances; S(2) makes contacts of 3.277(1) and 3.148(1) Å to Cl at $(\frac{1}{2}, \frac{1}{2}, \frac{1}{2})$ and $(\frac{1}{2}, \frac{1}{2}, 0)$ respectively and S(3) makes contacts to the same Cl of 3.243(1) and 3.279(1) Å. The shorter distance to S(1) is 3.659(1) Å to Cl at (0, 0, 0); this is close to the sum of the van der Waals radii (3.6 Å). The cation is thus bound to four anions by eight close contacts and these interactions prevent disorder in $[S_5N_5]Cl$.

Recently, correlation functions relating bond angles at nitrogen to adjacent bond lengths have been proposed.[25] The relevant functions for cations are given below where d is in pm

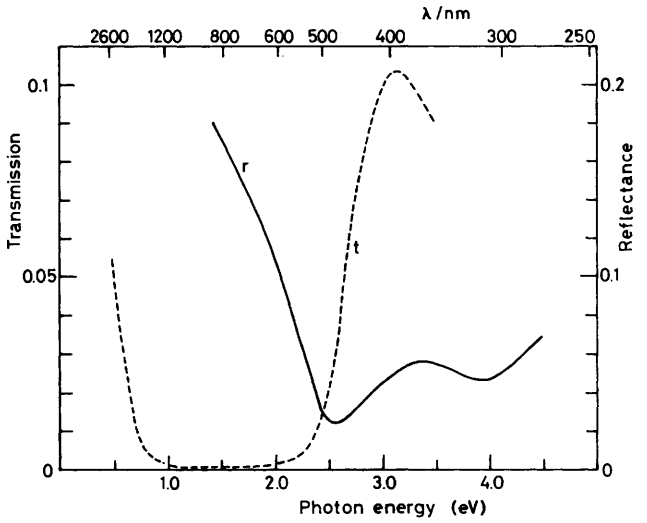

Figure 6. Transmission (t) and reflectance (r) spectra of vacuum-deposited $(SN)_x$ films (thickness *ca.* 0.2 and 1.0 μm) on a microscope slide using electrochemically prepared $(SN)_x$ as source material for deposition. The reflectance spectrum exhibits the characteristic plasma edge terminating at *ca.* 2.5 eV [value comparable with films obtained from classical $(SN)_x$ (*i.e.* from S_2N_2)]

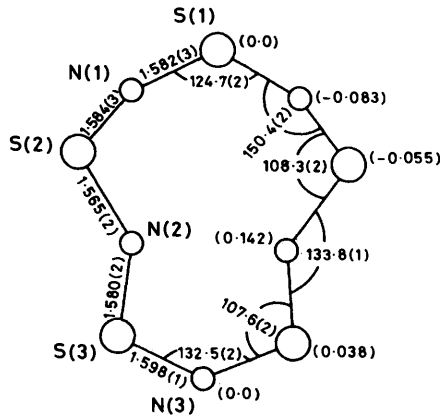

Figure 7. The geometry of the $S_5N_5^+$ cation in $[S_5N_5]Cl$. Bond lengths (Å) and angles (°) are shown with e.s.d.s. Distances (Å) from the plane $1.38x + 6.690z = 1.745$ are given in parentheses

$$d(\text{NS}) = 187.03 - 0.2263\hat{N}$$

$$d(\text{SN}) = 213.00 - 0.4861\hat{S}$$

and angles at S and N ($\hat{S}$ and $\hat{N}$) are in degrees. The correlations can be used to rationalize ring geometries and to detect distortions arising from secondary interactions.[25] For the cation in $[S_5N_5]Cl$, the observed mean bond length is 1.582(2) Å [158.2(2) pm] and the mean bond angles are SNS 140.2(2) and NSN 111.3(2)°. Mean structural parameters calculated by the MNDO method (d = 154.4 pm, $\hat{N}$ = 143.9 and $\hat{S}$ = 109.4°) compare well with these values. The bond angles deduced from the above equation, and corresponding to the observed mean bond length, are $\hat{N}$ = 127.4 (±1.4)°* and $\hat{S}$ = 112.7 (±3.0)°*

* These errors were calculated according to the procedure described in ref. 25. The errors take into account both the deviations of the true values from linearity and also the *X*-ray experimental errors (the true values being those that would be obtained from a 'perfect' *X*-ray structure determination).

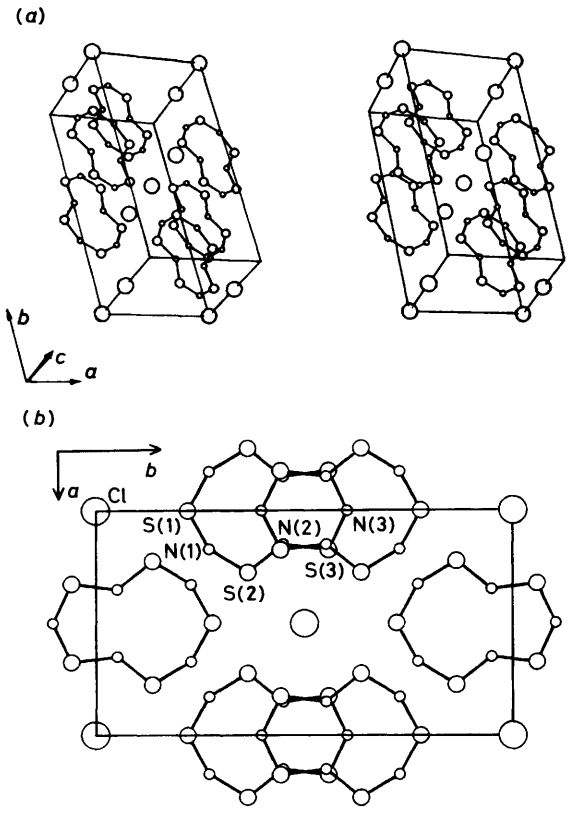

Figure 8. Contents of the unit cell of $[S_5N_5]Cl$. (*a*) Stereoview (the origin of the unit cell is at the bottom left corner). (*b*) View parallel to *c* axis with atom labelling of the asymmetric unit (The labelled chloride ion is at a distance *c*/2 above the origin of the unit cell)

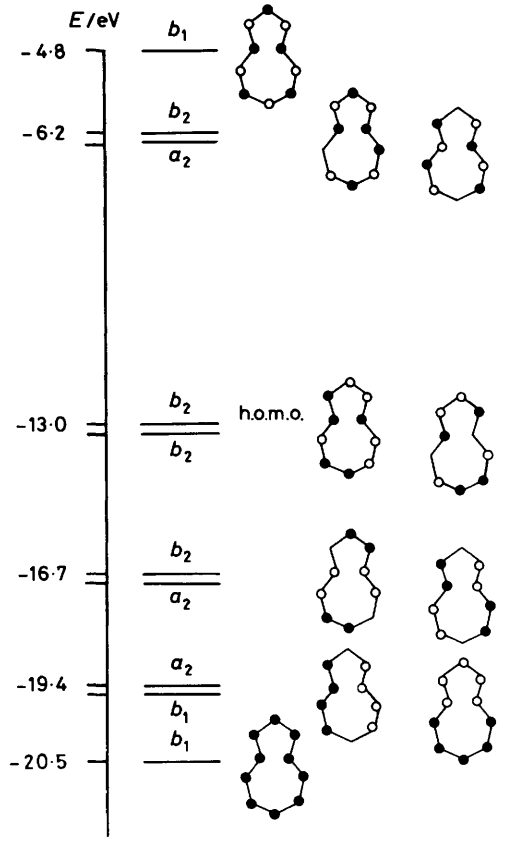

Figure 9. MNDO-Calculated π-orbital energy scheme for $S_5N_5^+$

indicating appreciable bond compression in the ring. Comparison with the S–N bond lengths found in previously reported, disordered, $S_5N_5^+$ salts is not possible because disordered structure solutions correspond to a statistical combination of the solid-state structures.

The deviations observed in $[S_5N_5]Cl$ may be ascribed in part to ring strain and also to electron drift from the chloride ion into a low-energy unoccupied π* orbital (see Figure 9), which causes a corresponding weakening and lengthening of the bonds and lowering of the energy gap between the lowest unoccupied and highest occupied molecular orbitals (l.u.m.o.–h.o.m.o.). This mechanism may also account for the bright red colour of $[S_5N_5]Cl$ compared with the usual yellow, since the interaction of the Cl^- ion with the l.u.m.o. would perturb the π-system of the cation. If the h.o.m.o.–l.u.m.o. gap diminishes as a result, the u.v.–visible absorption would shift to longer wavelengths and the compound would appear more red. On addition of SO_2 to the salt, the chloride ion co-ordinates preferentially to the solvent and the yellow colour of the $S_5N_5^+$ ion is restored (see above).

Electronic Structure of $[S_5N_5]Cl$.—The electronic spectrum of the $S_5N_5^+$ cation has previously been investigated at the π-electronic PPP level,[26] and the extended Hückel level.[27] A brief MNDO[28] study of the relative stability of various $S_5N_5^+$ isomers has also been published.[6] The $S_5N_5^+$ ion has been re-examined at the MNDO level in order to calculate its electronic structure and the geometry of the azulene type ring.

Two calculations were performed (see Figures 9 and 10) using as initial geometry in each case the bond lengths and ring angles observed in the structure of $[S_5N_5]Cl$ (and with the twist angles set to zero). In the first calculation the ring was constrained to a plane (C_{2v} symmetry) whilst in the second, the ring was allowed to buckle out of plane. The results from the two calculations were very similar. As the largest ring torsion angle calculated in the fully optimised case was only 3.6° and the difference in energy between the two calculations was only 0.155 kcal mol^{-1}, the following discussion will be in terms of the planar (C_{2v}) molecule.

In $S_5N_5^+$, the 54 valence electrons occupy ten σ-bonding orbitals and ten lone-pair orbitals, leaving 14 electrons to be distributed amongst seven π orbitals. The π orbitals are shown in Figure 9. The MNDO calculation predicts a slightly different ordering of orbitals than a previous extended Hückel study;[27] we find that the h.o.m.o. of the ion is a π-type orbital, with lone pair molecular orbitals lying at slightly lower energies than the h.o.m.o. and h.o.m.o.-1 (−15 compared to −13 eV). The MNDO program[28] allows configuration interaction calculations for the excited singlet to be performed; the m.o. energies computed can be used to predict the u.v.–visible spectrum of the species in question. These calculations for $S_5N_5^+$, however, failed to achieve self-consistency, although substantial agreement with published calculations[26,27] is anticipated since the PPP–CI calculations of Gleiter and Bartetzko[27] predict only minor changes in the electronic spectrum for different conformers of $S_5N_5^+$.

The calculated atomic charges and molecular geometry are shown in Figure 10. The calculated mean bond length is 154.4 pm and the calculated mean angle at nitrogen is 143.9°. These values are in very good agreement with those deduced using the correlation function (the function predicts a bond length of

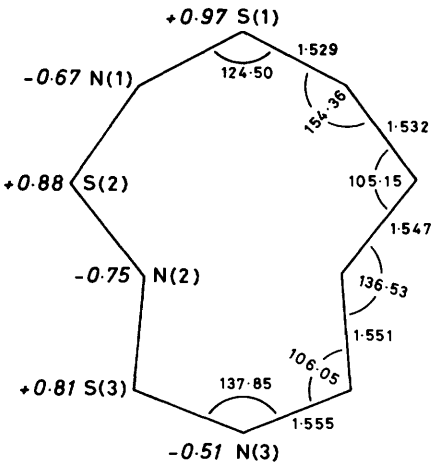

Figure 10. MNDO-Calculated atomic charges (in italics) and bond lengths (Å) and angles (°) for $S_5N_5^+$

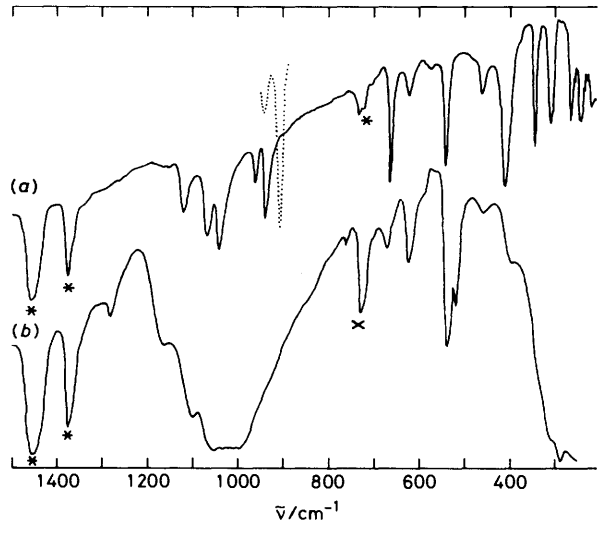

Figure 11. Infrared spectra of (*a*) $[S_5N_5]Cl$ (CsI plates) and (*b*) $[S_5N_5][BF_4]$ (KBr plates). (· · ·) Polystyrene marker (906.7 cm^{-1}), (✱) Nujol absorption, (×) eclipsed Nujol absorption

154.5 pm for a bond angle of 143.9°). The MNDO values are within 0.2 of an e.s.d. of the correlation function and thus the value of both approaches in predicting minimum energy conformation is confirmed.

Experimental

General.—All manipulations of solids were performed in an atmosphere of dry nitrogen in a Vacuum Atmospheres Co. glove-box (HE43–2). Glassware was dried before use either in an annealing oven (*ca.* 500 °C) or by flaming with a hand torch. The closed extractor used in purifications has been described previously;[22] the Schlenk tubes used in the reactions were modified so as to enable work under overpressure (liquid SO_2) and vacuum (*i.e.*, no ground joints) and were fitted with Rotaflo valves instead of greased taps. The filtration bridge (horizontal portion) connecting the two vertical limbs of the Schlenk tube was fitted with a sealed-in 20-mm diameter Pyrex sinter of suitable porosity.

Where necessary the reaction was thermostatted with a Haake refrigerated bath circulator (type F2). Volatiles were manipulated in a Monel vacuum manifold, equipped with Whitey valves (1KS4) and a stainless-steel Bourdon pressure gauge. Infrared spectra were run as Nujol mulls between KBr or CsI plates on a Perkin-Elmer PE577 spectrophotometer. Raman spectra of solids were recorded on a Cary 82 spectrophotometer using the exciting line at 5 145 Å. Differential scanning calorimetry measurements were made on a Mettler FP85 thermal analysis cell coupled to a Mettler FP80 processing unit and a Vitatron 2001 y-t chart recorder. Potentiostatic electrolyses were performed using an H. B. Thompson Ministat precision potentiostatic current source and cyclic voltammograms were recorded using a Bioanalytical Systems Inc. CV-1B cyclic voltammetry instrument coupled to a Linseis 1700 x-y chart recorder.

Starting Materials.—The compounds $[S_5N_5][FeCl_4]$ and $[S_5N_5][AlCl_4]$ were prepared according to the literature methods;[29] CsF (Ventron) was heated *in vacuo* above 200 °C for 6 h before use. Liquid SO_2 (BDH) was distilled from P_4O_{10} and stored in a stainless-steel container over CaH_2. Acetonitrile was purified according to the procedure of Walter and Ramaley.[30] Tetrahydrofuran (Koch-Light) was purified by distillation from sodium wire and stored under nitrogen. $LiClO_4$ (BDH) was fused under a stream of dry nitrogen for 3 h and stored under dry nitrogen. HBF_4 (50% aqueous) (Koch-Light) was used without further purification.

Preparation of $[S_5N_5]Cl$.—(*a*) *From* $[S_5N_5][FeCl_4]$ *and* CsF. The compound $[S_5N_5][FeCl_4]$ (1.0 g, 2.3 mmol) ground together with CsF (1.07 g, 7.0 mmol) was placed with a Teflon-coated magnetic stirring bar in one bulb of a modified Schlenk tube. Sulphur dioxide (*ca.* 10 cm^3) was condensed in and stirring was continued at room temperature for 16 h. The resulting mixture was filtered and the insolubles were washed with SO_2 distilled back from the solubles until pale grey. The SO_2 was removed to yield red-orange crystalline solubles (crude $[S_5N_5]Cl$) and grey powdery insolubles (FeF_3,CsCl). The crude $[S_5N_5]Cl$ was placed in a closed extractor and extracted with acetonitrile (48 h) to yield $[S_5N_5]Cl$ as a scarlet-red microcrystalline insoluble solid, and a mixture of S_4N_4, $[S_5N_5][FeCl_4]$, and CsCl as the soluble impurities extracted by acetonitrile. Yield 0.43 g, 69%. I.r.: $\nu_{max.}$ at 1 120s, 1 070s (sh), 1 045s, 965m, 945m, 735w, 705vw, 670m, 625m, 585vw, 540s, 460m, and 410s cm^{-1}. Raman: $\nu_{max.}$ at 730w, 695w, 670vw, 645s, 590w, 560vw, 465s, 415vw, 320w, 260m, 220s, 195m, 145s, 100m (sh), 95m, 55vs, and 45vs cm^{-1} (Found: Cl, 13.6; N, 26.2; S, 59.9. Calc. for ClN_5S_5: Cl, 13.3; N, 26.35; S, 60.3%).

(*b*) *From* $[S_5N_5][AlCl_4]$ *and* thf. On shaking $[S_5N_5][AlCl_4]$ (0.46 g, 1.15 mmol) with dry thf (2 cm^3, 24.7 mmol) the orange colour of the tetrachloroaluminate was immediately replaced by the deep red colour of $[S_5N_5]Cl$. After leaving to stand for *ca.* 5 min another 3 cm^3 of thf were added. No further change was observed and the solid was filtered off, washed with thf (2 cm^3) and dried *in vacuo*. Yield 0.255 g, 83% (Found: Cl, 13.2; N, 26.4; S, 60.4. Calc. for ClN_5S_5: Cl, 13.3; N, 26.3; S, 60.3%). I.r. (Figure 11): $\nu_{max.}$ at 1 122m, 1 070m, 1 043m, 963w, 942m, 735w, 668s, 623w, 580vw, 542s, 462w, 411s, 347s, and 311s cm^{-1}.

Preparation of $[S_5N_5][BF_4]$.—The compound $[S_5N_5]Cl$ (2.2 g, 8.3 mmol) was placed in a Polythene flask and cold (−15 °C) HBF_4(aq) (25 cm^3) was syringed on top. After shaking briefly at room temperature in an ultrasonic bath, the mixture was left overnight at −15 °C. It was then filtered under reduced pressure in a polyethylene filtration apparatus using Zitex extra-fine Teflon filter membranes. The resulting orange

crystalline solid was washed (3 × 1 cm^3) with cold diethyl ether and extracted (closed extractor) with pentane for 24 h to remove S_4N_4 (0.1 g). The remaining solid was extracted briefly (30 min) with acetonitrile to yield an orange crystalline solid as the soluble product. Yield 1.6 g, 61.5%. I.r. (Figure 11): $\nu_{max.}$ at 1 282w, 1 165w (sh), 1 102w (sh), *ca.* 1 060—1 000vs vbr, 765vw, 730s, 675w, 625m, 565vw, 539s, 520s, 460w, and 395w cm^{-1}. Raman: $\nu_{max.}$ at 580m, 533vs, 482m br, 422m, 262s, 238m, and 195vs cm^{-1} (Found: B, 3.45; N, 21.4; S, 50.0. Calc. for $BF_4N_5S_5$: B, 3.4; N, 22.1; S, 50.55%).

Tensimetric Titration of $[S_5N_5]Cl$ *with* SO_2.—A small flask, fitted with a Rotaflo valve and containing $[S_5N_5]Cl$ (0.1928 g), was connected *via* a T-piece and Whitey valve to a mercury-in-glass manometer and the Monel vacuum manifold. The flask was maintained at 2 °C in an alcohol bath. A little SO_2 was condensed in, and after allowing 5 min for the $[S_5N_5]Cl$ to soak, the SO_2 was carefully removed until no more liquid was present and only the yellow microcrystalline solvate was present. After allowing 15 min for equilibration the pressure of the system was measured and the Rotaflo flask was detached from the manometer and weighed. On reattachment, a small amount of SO_2 was removed and the process was repeated. It was found that final equilibration was not achieved even after 4 h and so a standard time of 15 min was allowed for each reading. Solvate formation required initiation by exposure to an excess pressure of SO_2; it was not formed by addition of small aliquots of SO_2 to pure $[S_5N_5]Cl$.

Electrochemical Studies of $S_5N_5^+$.—(*a*) *Cyclic voltammetry* (*c.v.*). The cell used is shown in Figure 2. The working electrode (4) consisted of a platinum disc mounted in glass (area 1.47 mm^2) and a coiled platinum wire formed the auxiliary electrode (5). The reference electrode (r.e., 3) was suitable for liquid SO_2 (up to *ca.* 3 atm overpressure) and for other non-aqueous solvents. It was composed of a silver gauze at the upper end in a glass bulb, and a connecting glass tube (outside diameter ¼ in) closed at its lower end with a dense frit which served as a liquid junction. The entire volume of the r.e. was filled with $AgNO_3$ (0.01 mol dm^{-3})–$LiClO_4$ (0.1 mol dm^{-3})–acetonitrile solution. Its potential *vs.* the s.c.e. was +0.26 V (at 18 °C). The cyclic voltammograms of $[S_5N_5][BF_4]$ in MeCN obtained with a directly inserted Ag/Ag^+ r.e. (3) were checked against s.c.e. connected to the cell *via* a salt bridge. The salt bridge was made of semi-rigid FEP tubing (outside diameter ¼ in) provided at both ends with thermally sealed-in ceramic wicks and filled with 0.1 mol dm^{-3} $[NBu_4][BF_4]$ in MeCN. The results obtained by both arrangements were in very good agreement: ±10 mV. The r.e. (3) was kept in a special storage vessel under dry nitrogen in contact with a reservoir of $AgNO_3$–$LiClO_4$–MeCN solution of the same concentration as the electrolyte within. The storage vessel also enabled the topping up of the electrolyte inside the r.e. (by a combination of tipping, freezing, and evacuation).

The procedure for c.v. in liquid SO_2 was as follows. The ¼-in port (6) for the r.e. of the cell was closed with a stopper and the solids ($[S_5N_5]Cl$ and $[NBu_4][BF_4]$) and a stirring bar were put into the cell in a glove-box. The cell was evacuated and SO_2 was condensed in at *ca.* −15 °C. The stopper was quickly replaced with the r.e. (3) under a counter-flow of nitrogen. The preparation for c.v. in acetonitrile was simpler: after the solids $[S_5N_5][BF_4]$ and $[NBu_4][BF_4]$ (or $LiClO_4$) were put into the cell in a glove-box the desired amount of MeCN was injected into the cell using a gas-tight syringe against a counter-flow of nitrogen. Recorded background scans +2.0 to 0.0 V for SO_2 and +1.5 to −1.5 V *vs.* s.c.e. for MeCN showed no significant peaks.

(*b*) *Potentiostatic electrolysis of* $[S_5N_5][BF_4]$. A three-electrode divided cell very similar in construction to that described above (Figure 2) was used. The reference and working electrode compartment was separated from the auxiliary electrode compartment by a medium porosity glass frit. The working electrode was a platinum sheet (area 4.0 cm^2). $[S_5N_4][BF_4]$ (0.25 g, 0.79 mmol) was dissolved in $LiClO_4$ (0.1 mol dm^{-3})–MeCN (40 cm^3) in the cell and the electrodes were inserted. The whole apparatus was maintained under dry nitrogen (1 atm) at 0 °C. The electrodes were connected to the potentiostatic current source and at the working electrode potential were maintained at −0.26 V, with a current of approximately 0.3 mA. A compact bronze layer deposited on the working electrode. Electrolysis was stopped after 2.5 h.

In a further experiment, the working electrode was glass coated with vapour-deposited $(SN)_x$ and gripped in platinum jaws. With the same cell solution as before, a potential of 0 V *vs.* s.c.e. was maintained for 4.5 h; the current remained steady at 0.22 ± 0.02 mA throughout. The current yield (50%) was estimated from the layer thickness (see Discussion section).

Table 2. Fractional co-ordinates (× 10^4) for $[S_5N_5]Cl$

Atom	*x*	*y*	*z*
Cl	0	0	5 000
S(1)	0	2 207(1)	2 500
S(2)	2 750(1)	3 642(1)	2 039(1)
S(3)	1 751(1)	5 576(1)	2 103(1)
N(1)	1 720(3)	2 718(2)	2 281(5)
N(2)	1 505(3)	4 485(2)	2 001(4)
N(3)	0	6 024(2)	2 500

Thermal Stability of $[S_5N_5]Cl$.—(*a*) *Raman studies.* A small amount of $[S_5N_5]Cl$ was sealed under nitrogen in a capillary tube and heated to 95 °C for a few minutes. A Raman spectrum was recorded of the red-orange involatile material at the bottom of the tube. The experiment was repeated, heating to 127 °C and Raman spectra were recorded of the resulting yellow involatile solid at the bottom of the tube and the yellow volatile which had collected at the top of the tube; unassigned peaks are indicated (?). Red-orange melt (95 °C): 465m (?), 350w (S_4N_4), 285m (sh) (?), 275m (sh) (?), 260m (sh) ($[S_4N_3]Cl$), 250m (sh) ($[S_4N_3]Cl$), 220m (S_4N_4), 115s (sh) {$(NSCl)_3$, $[S_4N_3]Cl$}, 70vs {$(NSCl)_3$, $[S_4N_3]Cl$}, 45vs (sh) (S_4N_4, $[S_4N_3]Cl$), 35vs (?), 30vs (?), 15vs cm^{-1} (?). Yellow involatile solid (127 °C): 1 000w (?), 720w (S_4N_4), 605m ($[S_4N_3]Cl$), 560m ($[S_4N_3]Cl$), 450s ($[S_4N_3]Cl$), 250m ($[S_4N_3]Cl$), 215s (S_4N_4), 200s (S_4N_4), 165vw ($[S_4N_3]Cl$), 150w ($[S_4N_3]Cl$), 110s (sh) ($[S_4N_3]Cl$), 100s ($[S_4N_3]Cl$), 80s ($[S_4N_3]Cl$), 45vs ($[S_4N_3]Cl$, S_4N_4), 25w cm^{-1} (?). Yellow volatile solid (127 °C): 1 125w, 700vw br, 620w br, 485w, 435w, 375m, 340s, 320m, 195m, 180s, 110s, 80vs, 40w, 25m cm^{-1}. All modes can be assigned to $(NSCl)_3$.

(*b*) *Differential scanning calorimetry.* In a typical experiment $[S_5N_5]Cl$ (5.98 mg) was hermetically sealed under dry nitrogen in an aluminium capsule by cold welding in a press. The sample was then heated in a thermal analysis cell (rate 4 °C min^{-1}, initial temperature 48 °C, final temperature 120 °C) and the d.s.c. trace recorded on a y-t chart recorder. Infrared spectra showed that the yellow residue was a mixture of S_4N_4 and $[S_4N_3]Cl$. Typical weight changes during thermolysis were <0.03 mg.

Crystal Growth and Crystallography of $[S_5N_5]Cl$.—A small amount (*ca.* 200 mg) of $[S_5N_5]Cl$ was placed on the frit of a closed extractor[22] and acetonitrile (10 cm^3) was distilled into the bulb; the $[S_5N_5]Cl$ was extracted for 4 d. Small translucent scarlet platelets formed alongside the path of the refluxing

solvent below the frit. Suitable crystals were selected by hand and sealed under nitrogen in quartz capillaries.

Crystal data. ClN_5S_5, M = 265.8, monoclinic, space group $C2/c$, a = 7.98(1), b = 14.37(1), c = 7.30(1) Å, β = 97.15(5)°, U = 830.6 Å^3, Z = 4, D_c = 2.12 g cm^{-3}, $F(000)$ = 532, λ(Mo-K_α) = 0.7107 Å, μ = 1.53 mm^{-1}.

Intensity data from a crystal of dimensions 0.25 × 0.2 × 0.15 mm were collected for the layers l = 0—10 on a Stoe STADI-2 automatic two-circle diffractometer using graphite-monochromatised Mo-K_α radiation. Absorption and extinction corrections were not applied; 1 758 reflections were measured of which 1 629 were unique with an internal agreement R = 0.0086. For refinement of the structure 1 366 reflections for which $I > \sigma(I)$ were used. All calculations were carried out using the SHELX 76 suite of programs.[31]

Structure determination. The direct-methods program EEES yielded a solution of the phase problem. The resulting E map showed an atom on a centre of symmetry, interpreted as Cl; two atoms on a two-fold axis of the space group and four other atoms in general positions were interpreted as the S_5N_5 fragment with two-fold axial molecular symmetry. Refinement of positional and thermal parameters proceeded by full-matrix least-squares methods until the shifts were less than 0.01 of the corresponding e.s.d. and R was 0.054. At an intermediate stage individual scale factors for the data collection layers were refined and subsequently fixed at the refined values. It was noted that the values of U_{33} for the atoms of the cation were larger than the values of U_{11} and U_{22}, suggesting that lower symmetry might be involved, *i.e.*, the two-fold axis of S_5N_5 was an approximation only. A number of models were investigated in order to refine the structure in the lower-symmetry space group Cc; none of these reduced the magnitudes of U_{33} and all gave considerably worse e.s.d.s of all parameters. For the final refinement the space group $C2/c$ was retained; the atomic co-ordinates are given in Table 2. The final weighting scheme was $w = 2.52/[\sigma^2(F) + 0.000\,65\,F]$. The atomic scattering factors used were taken from International Tables.[32]

Acknowledgements

We thank the S.E.R.C. for a research grant (to A. J. B. and Z. V. H.) and for a studentship (to A. G. K.). We also thank Dr. O. R. Brown, School of Chemistry, University of Newcastle upon Tyne, for valuable discussion, Dr. G. Russell, Department of Applied Physics and Electronics, University of Durham, for s.e.m. and r.e.d. photographs, Dr. R. H. Friend, Cavendish Laboratory, University of Cambridge, for $(SN)_x$ optical spectra, Mr R. C. Coult for analyses, and Mr. I. B. Gorrell (supported by an S.E.R.C. research grant) for his invaluable technical assistance.

References

1 H. W. Roesky and W. G. Bowing, *J. Chem. Soc., Chem. Commun.*, 1975, 735.
2 A. J. Banister, J. A. Durrant, I. Rayment, and H. M. M. Shearer, *J. Chem. Soc., Dalton Trans.*, 1976, 929.
3 A. Hazell and R. G. Hazell, *Acta Chem. Scand.*, 1972, **26**, 1987.
4 P. Klinzing, W. Willing, U. Müller, and K. Dehnicke, *Z. Anorg. Allg. Chem.*, 1985, **529**, 35.
5 A. J. Banister and J. A. Durrant, *J. Chem. Soc.*, 1978, (*S*) 152, (*M*) 1931.
6 R. Gleiter and R. Bartetzko, *Z. Naturforsch., Teil B*, 1981, **36**, 956.
7 A. J. Banister, Z. V. Hauptman, and A. G. Kendrick, *J. Chem. Soc., Chem. Commun.*, 1983, 1016; A. J. Banister, Z. V. Hauptman, and A. G. Kendrick, U.S.P. 4 555 316/1985; B.P. 2 147 889B/1986.
8 L. Zbořilová and P. Gebauer, *Z. Chem.*, 1979, **19**, 32.
9 H. B. Mark and K. J. Mulligan, *Chem. Eng. News*, 1984, **62(5)**, 4.
10 D. F. Burow, *Inorg. Chem.*, 1972, **11**, 573.
11 P. J. Elving, J. M. Markowitz, and I. Rosenthal, *J. Phys. Chem.*, 1961, **65**, 680.
12 L. A. Tinker and A. J. Bard, *J. Am. Chem. Soc.*, 1979, **101**, 2316; A. J. Bard, *Inorg. Chem.*, 1983, **22**, 2689.
13 H. P. Fritz and R. Bruchhaus, *Z. Naturforsch., Teil B*, 1983, **38**, 1375.
14 M. M. Beizer (ed.), 'Organic Electrochemistry,' Dekker, New York, 1973.
15 P. Castellonese and P-C. Lacaze, *C. R. Acad. Sci.*, 1972, **274**, 2050.
16 R. J. Nowak, C. J. Loyal, and D. C. Weber, *J. Electroanal. Chem.*, 1983, **143**, 413.
17 D. Knittel, *J. Electroanal. Chem.*, 1985, **195**, 345.
18 T. Chivers and M. Hojo, *Inorg. Chem.*, 1984, **23**, 1526.
19 Z. V. Hauptman, unpublished work.
20 A. J. Banister, Z. V. Hauptman, J. Passmore, P. S. White, and C. M. Wong, *J. Chem. Soc., Dalton Trans.*, 1986, 2371.
21 A. A. Bright, M. J. Cohen, A. F. Garito, A. J. Heeger, C. M. Mikulski, P. J. Russo, and A. G. MacDiarmid, *Phys. Rev. Lett.*, 1975, **34**, 206.
22 R. W. H. Small, A. J. Banister, and Z. V. Hauptman, *J. Chem. Soc., Dalton Trans.*, 1984, 1377.
23 D. D. Wagman, W. H. Evans, V. B. Parker, I. Harlow, S. M. Bailey, and R. H. Schumm, 'Selected Values of Chemical Thermodynamic Properties,' Nat. Bur. Stand., Technical Note 270-3, U.S. Government Printing Office, Washington, D.C., 1968.
24 R. J. Gillespie, J. F. Sawyer, D. R. Slim, and J. D. Tyrer, *Inorg. Chem.*, 1982, **21**, 1296.
25 A. J. Banister, I. B. Gorrell, and R. S. Roberts, *J. Chem. Soc., Faraday Trans. 2*, 1985, 1783.
26 R. Zahradník, A. J. Banister, and H. G. Clarke, *Collect. Czech. Chem. Commun.*, 1973, **38**, 998.
27 R. Gleiter and R. Bartetzko, *Inorg. Chem.*, 1978, **17**, 995.
28 M. J. S. Dewar and W. Thiel, *J. Am. Chem. Soc.*, 1977, **99**, 4899; 4907.
29 A. J. Banister and H. G. Clarke, *Inorg. Synth.*, 1977, **17**, 188.
30 M. Walter and C. Ramaley, *Anal. Chem.*, 1973, **45**, 163.
31 G. M. Sheldrick, SHELX program for *X*-ray crystal structure determination, University of Cambridge, 1976.
32 'International Tables for Crystallography,' Kynoch Press, Birmingham, 1974, vol. 4.

Received 21*st May* 1986; *Paper* 6/986